

## Performance Assessment of Polycrystalline Silicon Pv Modules in Low Latitude Regions as A Function of Temperature

**P.E. Ugwuoke, PhD**

National Centre for Energy Research and Development  
University of Nigeria  
Nsukka.

**C.E. Okeke, PhD**

Department of Physics and Astronomy  
University of Nigeria  
Nsukka.

### Abstract

The performance of any PV module is directly proportional to the solar irradiance impinging on its surface and having enough energy capable of releasing electrons from the valence level to the conduction level of the cells of the module. It has been observed that module performance is significantly hampered by thermal stress due to temperature variations during operation under natural environment. A one-year performance characteristics of a 50-Watt polycrystalline silicon PV module as a function of temperature at Nsukka in Nigeria (Lat. 6° 52') was evaluated and reported in this paper. Significant decrease in efficiency  $Eff$ , maximum voltage  $V_{max}$ , open-circuit voltage  $V_{oc}$  and fill factor  $FF$  was noticed with increase in the module temperature at irradiances above 600 W/m<sup>2</sup> while maximum current  $I_{max}$  and short-circuit current  $I_{sc}$  showed no noticeable effect of the module temperature rise. At an irradiance of 1000W/m<sup>2</sup> and a module temperature of 45°C, the maximum power output of the module was observed to be 28.84 Watts, which is approximately 58 % of the manufacturer's specification. The module performance ratio (MPR) at irradiance of 600W/m<sup>2</sup>, defined as the ratio of effective efficiency to the efficiency at standard test condition (STC), was observed to be 76.75% and decreased appreciably to 60.71% at 1000W/m<sup>2</sup>.

**Key Words:** Performance Variation, Temperature effects, Polycrystalline Silicon, Photovoltaic modules, Low Latitude.

### 1. Introduction

The PV module output ratings and operation specifications are usually determined by solar PV module manufacturers in their cold and temperate environments under simulated and steady-state sunlight conditions. These specifications are designated "Standard Test Conditions" (1000W/m<sup>2</sup> irradiance, 25°C cell temperature and air mass of 1.5 global spectrum). However, when deployed in the field, the performances are bound to vary from the stipulated specifications because the solar intensity is both location and time dependent and is usually highly modulated due to the rapidly changing cloud cover and dust haze. This leads to variations in ambient and module temperatures [1].

Temperature has a non-negligible effect on the PV module characteristics. The short-circuit current will increase slightly with increasing module temperature  $T_{mod}$ . This increase in the short-circuit current arises from a decrease in the band-gap energy  $E_g$  of the material as the temperature increases according to [2].

$$E_g(T) = E_g(0) - \frac{\alpha T^2}{T+b} \quad \text{-----} \quad (1)$$

Band gap energy of silicon,  $E_g(0) = 1.16 \text{ eV}$ ,  $\alpha = 7 \times 10^{-4} \text{ eVK}^{-1}$  and  $b = 1100\text{K}$ .

But short-circuit current  $I_{sc} = I_0 \left[ \exp\left(\frac{qV_{oc}}{KT}\right) - 1 \right] \quad \text{-----} \quad (2)$

Where  $I_0 = \text{saturation current} = A_0 T^3 \exp\left(-\frac{E_g}{KT}\right) \quad \text{-----} \quad (3)$

The open-circuit voltage  $V_{oc}$  would decrease linearly with increase in module temperature because of the exponential increase in saturation current[2].

## 2. Experimental Procedures

The 50-Watt polycrystalline silicon PV module and the temperature sensors were installed on an elevated support structure at 406 metres above sea level [3]. The module was tilted at approximately  $22^{\circ}$  to the horizontal and south-facing. The investigation was performed for a period of one year, spanning from November 2004 to October 2005 at the grounds of Energy Research Centre, University of Nigeria, Nsukka. The module has the following nominal parameters at STC:

❖ No. of cells per module	=	36 cells of 4 parallel and 9 series strings
❖ Maximum rated power	=	50 $W_p$
❖ Maximum rated voltage	=	17.20 V
❖ Maximum rated current	=	2.90 A
❖ Open-circuit voltage	=	20.00 V
❖ Short-circuit current	=	3.20 A
❖ Surface Area	=	0.38 $m^2$
❖ Make	=	Tessag Solar Industries, USA

The sensors are connected directly to a software-based CR10X Campbell Scientific data logger, while the module is connected to the logger via a voltage divider. Instantaneous data collection were performed by the logger at intervals of 5 minutes and averaged over 10 minutes. Data download at the data acquisition site was performed every 10 days to ensure effective and accurate monitoring of the data acquisition system (DAS). The global solar radiation was monitored using a solar radiation sensor called SENSOL-MONOKRISTALLIN, manufactured by IKS PHOTOVOLTAIK Company in Western Germany, with calibration of  $60.6mV/1000Wm^{-2}$ . The ambient temperature was monitored using a Campbell Scientific temperature sensor. The back-surface temperature of the module was monitored using copper-constantan thermocouples.

## 3. Results and Discussion

Module performance response to temperature variations was monitored in terms of open-circuit voltage  $V_{oc}$ , short-circuit current  $I_{sc}$ , voltage at maximum power  $V_{max}$ , current at maximum power  $I_{max}$ , maximum power  $P_{max}$  and efficiency  $E_{ff}$ . In order to further determine the rate of variation of module response variables with module temperature, a linear statistical model  $Y = a + b(T_{mod} - 25)$  was fitted to the observed data to predict module performance at varying module temperatures, where the coefficient  $b$  is the rate of variation with respect to module temperature [4]. The temperature coefficients for currents  $\alpha$  and for voltages  $\beta$  of the module were subsequently evaluated as shown in figures 4 – 7. These temperature coefficients are simply the values of the coefficients of their fitting terms [5, 6]. Table 1 shows the annual average variation of open-circuit voltage, short-circuit current and module temperature under different meteorological conditions at different times of the day. It is observed here that the short-circuit current peaks at between 1200 hours and 1400 hours when the average irradiance and module temperatures are maximum, while the open-circuit voltage peaks around 1000 hours when the average irradiance is relatively moderate and average module temperature is close to ambient.

Figure 1 shows the I – V characteristics of the module as a function of module temperature. Here the increase in module temperature reduces the open-circuit voltage while the short-circuit current is noticed to be unaffected by the temperature rise.

Figures 2 and 3 show the average variation of open-circuit voltage and short-circuit current respectively with module temperature at different months of the year.

The maximum power, efficiency and fill factor were evaluated using the following expressions [7]:

$$\text{Max. Power } P_{max} = \frac{I_{max} V_{max}}{A E_e} \text{ ----- (4)}$$

$$\text{Fill factor FF} = \frac{I_{max} V_{max}}{I_{sc} V_{oc}} \text{ ----- (5)}$$

$$\text{Efficiency Eff} = \frac{I_{max} V_{max}}{P_{in}} = \frac{V_{oc} I_{sc} FF}{P_{in}} = \frac{V_{oc} I_{sc} FF}{A E_e} \text{ ---- (6)}$$

Where A is the module area.

On the basis of the data obtained and analysis performed, the module temperature was responsible for a significant percentage of the variations in all response variables of the module. However, the module temperature has a linear relationship with ambient temperature. It is the temperature difference between the module temperature and ambient temperature that influences the module performances significantly. The module temperature is noticed to be primarily dictated by the ambient temperature and irradiance, as could be seen in the strong correlation of module temperature with ambient temperature and irradiance. The ambient temperature sets the base temperature of the module while the irradiance predominantly sets the temperature rise of the module which is observed to be about  $0.015^{\circ}\text{C}$  per  $\text{Wm}^{-2}$ . In order to comprehensively evaluate the module performances over a reasonable time frame, it is important to predict the module temperature as a function of ambient temperature, wind speed, global irradiance and relative humidity. A mathematical model by Osterwald et al [8] to predict the module temperature,  $T_{\text{mod}}$  for the module as a function of ambient temperature  $T_a$ , wind speed, WS, global irradiance  $H_g$  and relative humidity RH, was fitted to the field monitored real data of these ambient parameters. The intended equation for the module temperature is given by [8]:

$$T_{\text{mod}} = K_1 H_g + K_2 T_a + K_3 RH + K_4 WS + C \text{ ----- (7)}$$

Using the NLREG data analysis software developed by P.H Sherrod [9], an empirical equation for the module temperature  $T_{\text{mod}}$ , was established as

$$T_{\text{mod}} (^{\circ}\text{C}) = 0.0355H_g + 0.705T_a + 0.0813RH + 1.807WS - 4.813 \text{ --- (8)}$$

Where  $K_1$ ,  $K_2$ ,  $K_3$  and  $K_4$  are coefficients which show the rate of variation of  $T_{\text{mod}}$  with  $H_g$ ,  $T_a$ , RH and WS. Table 2 is a correlation matrix showing the correlation of  $T_{\text{mod}}$  with  $H_g$ ,  $T_a$ , RH and WS while table 3 shows the summary of average performance response of the module as a function of different irradiance and module temperature levels.

#### 4. Conclusion

From the data analysis and performance evaluation of the polycrystalline module in our local environment, it was discovered that the maximum power output and efficiency of the module were significantly lower than their rated performances. At irradiance of  $1000 \text{ W/m}^2$ , the power output reduced by about 42.32% of the manufacturer's specification. Maximum efficiency of 9.67% was achieved at irradiance of  $600 \text{ W/m}^2$ . Module temperature was noticed to be significantly influential to the general performance of the modules. Open-circuit voltage  $V_{oc}$ , maximum voltage  $V_{\text{max}}$ , efficiency Eff and fill factor FF, were observed to be maximum in the mornings when module temperatures are low, while the short-circuit current  $I_{sc}$  and maximum current  $I_{\text{max}}$  were observed to be maximum in the afternoons when the insolation and module temperatures are highest.

#### References

1. **Atiku A.T. and Sambo A.S (1990)** "Experimental Characterization of Photovoltaic Solar Cells" Nig. J. Solar Energy Vol.9 pp 85 – 97.
2. **Del Cueto J.A. (2005)** "Closed-form Solutions and Parameterization of the Problem of Current-Voltage Performance of Polycrystalline Photovoltaic Modules Deployed at Fixed Latitude Tilt", Paper presented at the 31<sup>st</sup> IEEE Photovoltaic Specialists Conference and Exhibitions, Florida.
3. **Emery K (1996)** "Temperature dependence of Photovoltaic Cells, Modules and Systems", Proceedings of the 25<sup>th</sup> IEEE Photovoltaic Specialists Conference, pp1275 – 1278.
4. **King D.L. (1997)** "Temperature Coefficients for PV Modules and Arrays: Measurements, Methods, Difficulties and Results", Paper presented at the 26<sup>th</sup> IEEE Photovoltaic Specialists Conference, California.
5. **Lasnier F. and Gan Ang T. (1990)** "Photovoltaic Engineering Handbook", published under the Adam Hilger Imprint by IOP Publishing Company Ltd, England.
6. **Nsukka North-East Topographic Map, 1: 50,000; Sheet 287 NE (1963)**, published by the Federal Survey, Federal Republic of Nigeria.
7. **Onyegegbu S.O. (1989)** "Performance of Photovoltaic Cells in an Equatorial Climate", Solar and Wind Technology, Vol. 6 (3) pp 275 – 281
8. **Osterwald C. (2003)** "Photovoltaic Module Thermal/Wind Performance: Long-term Monitoring and Model Development for Energy Rating" NCPV and Solar Program Review, NREL pp 936 – 939.
9. **Sherrod P.H. (1991)** "NLREG – Non-linear Regression Analysis Program Version 6.3 (www.nlreg.com)

**Table 1. Annual Hourly Average Performance of the module.**

Time	Polycrystalline Module			T <sub>amb</sub> (°C)	Diffuse Irradiance (W/m <sup>2</sup> )	Global Irradiance (W/m <sup>2</sup> )	Wind Speed (m/s)
	V <sub>oc</sub>	I <sub>sc</sub>	T <sub>mod</sub>	T <sub>A</sub>	H <sub>d</sub>	H	W.S.
800	18.19	0.62	25.48	24.20	17.68	116.26	0.297
900	18.87	0.91	28.18	24.79	31.15	259.23	0.418
1000	19.02	1.45	30.44	25.85	37.54	402.65	0.449
1100	18.96	1.62	34.54	26.58	42.41	479.37	0.636
1200	18.83	1.91	36.59	27.52	46.81	521.02	0.581
1300	18.77	1.98	37.92	28.32	45.50	542.33	0.946
1400	18.74	1.84	38.51	29.29	43.03	502.51	0.806
1500	18.54	1.55	37.24	29.39	38.38	438.20	0.747
1600	18.43	1.21	34.59	29.37	33.47	318.44	0.732
1700	18.05	0.67	32.10	29.24	23.75	170.68	0.593
1800	16.53	0.28	29.18	28.58	9.62	52.30	0.209

**Table 2. Correlation Matrix of T<sub>mod</sub> with Ambient Parameters for the polycrystalline silicon module**

	Polycrystalline T <sub>mod</sub>
T <sub>mod</sub>	1.000
H <sub>g</sub>	0.9199
T <sub>a</sub>	0.9000
RH	- 0.4945
WS	0.3050

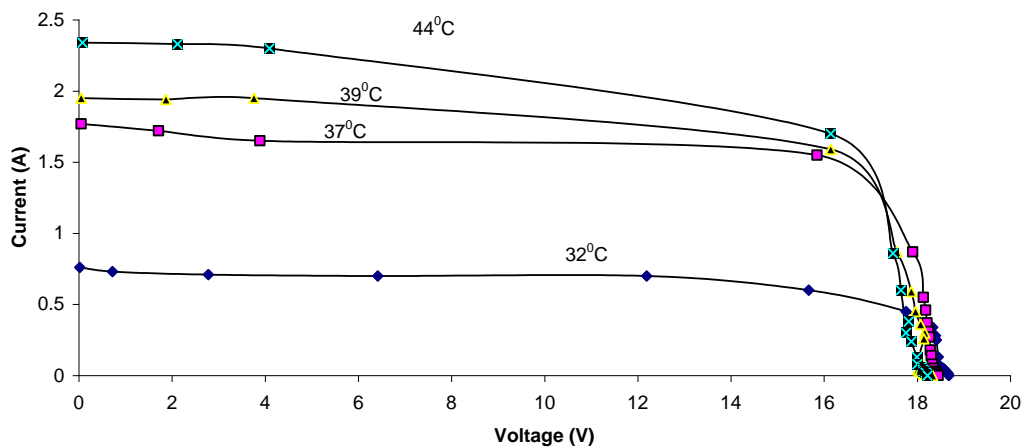


**Fig. 1. I - V Characteristics as a function of module temperature for the Polycrystalline Silicon PV Module**

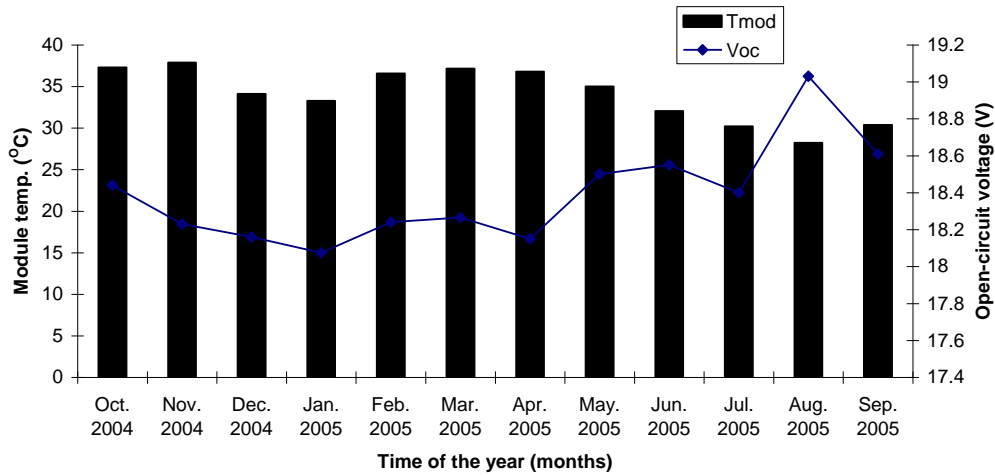


Fig. 2. Monthly Average variation of open-circuit voltage and module temperature for the Polycrystalline module

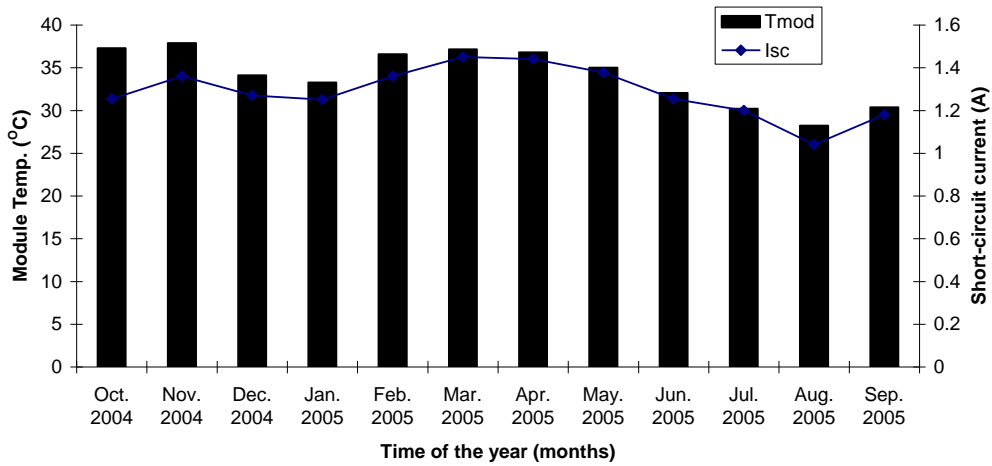


Fig. 3 Monthly Average variation of short-circuit current and module temperature for the Polycrystalline module

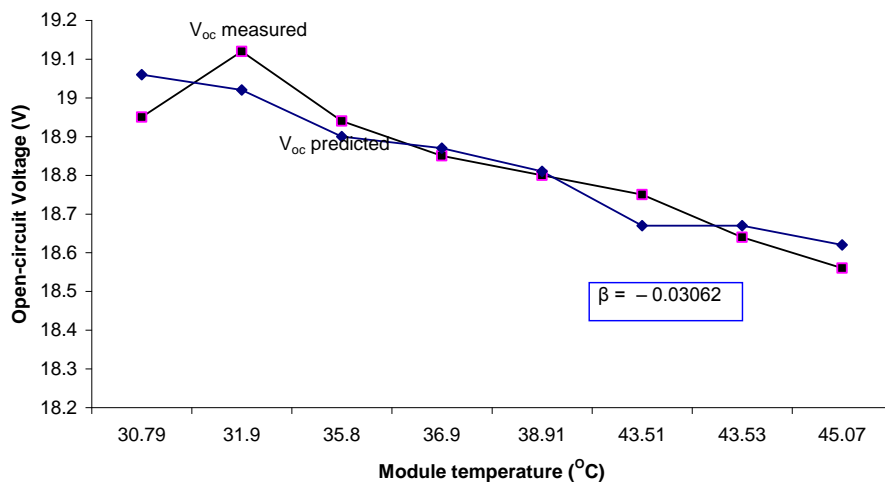
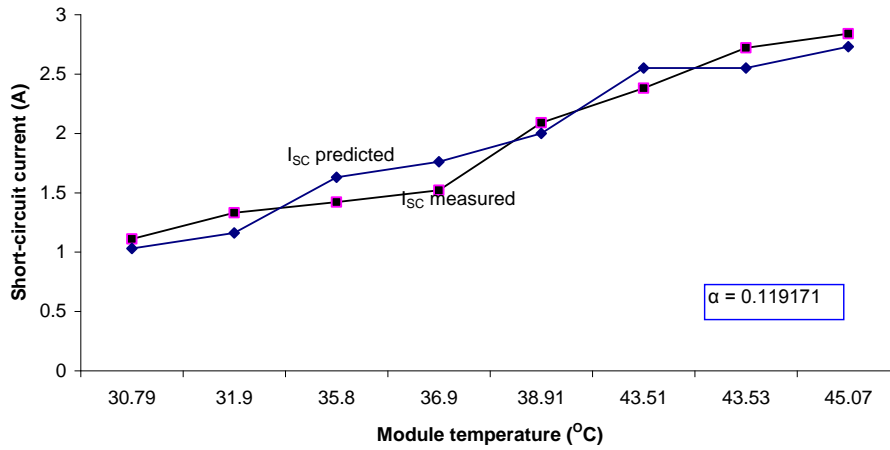
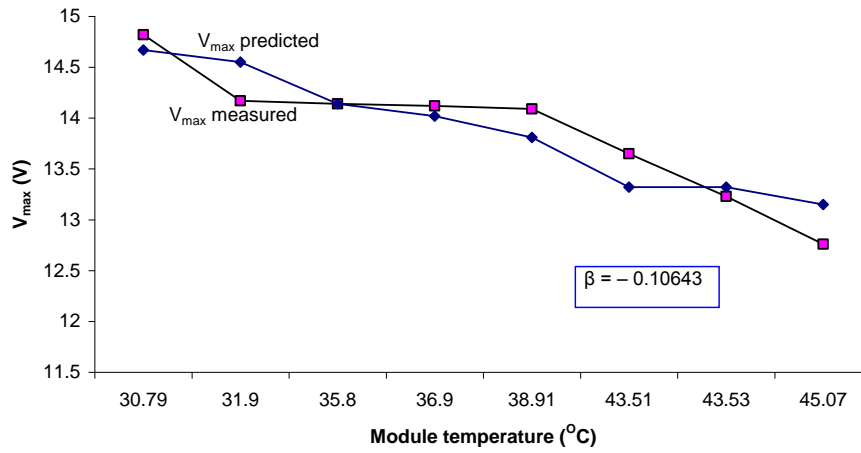


Fig. 4 Measured and predicted Voc as a function of module temperature for the polycrystalline module



**Fig. 5** Measured and predicted I<sub>sc</sub> as a function of module temperature for the polycrystalline module



**Fig. 6** V<sub>max</sub> measured vs V<sub>max</sub> predicted as a function of module temperature for the polycrystalline module

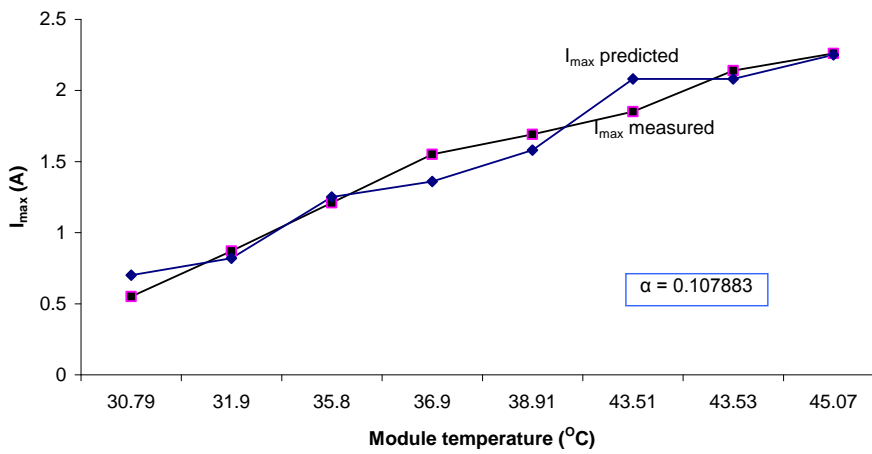


**Fig. 7** I<sub>max</sub> measured vs I<sub>max</sub> predicted as a function of module temperature for the polycrystalline module

**Table 3. Summary of Average Performance Response for the Polycrystalline PV module at different Irradiance and module temperature levels.**

<b>Glob. Irrad. H (W/m<sup>2</sup>)</b>	<b>Diffuse Irrad. H<sub>d</sub> (w/m<sup>2</sup>)</b>	<b>T<sub>amb</sub> (o<sup>c</sup>)</b>	<b>Wind Speed W.S. (m/s)</b>	<b>T<sub>mod</sub> (o<sup>c</sup>)</b>	<b>V<sub>oc</sub> (V)</b>	<b>I<sub>sc</sub> (A)</b>	<b>V<sub>max</sub> (V)</b>	<b>I<sub>max</sub> (A)</b>	<b>P<sub>max</sub> (W)</b>	<b>η (%)</b>	<b>FF (%)</b>
300	38.03	25.94	0.334	30.79	18.95	1.11	14.82	0.55	8.15	7.20	38.75
400	37.24	26.74	0.401	31.90	19.12	1.33	14.17	0.87	12.33	8.20	48.49
500	47.50	27.98	0.401	35.80	18.94	1.42	14.14	1.21	17.11	9.07	63.62
600	45.15	28.15	0.642	36.90	18.85	1.52	14.12	1.55	21.89	9.67	76.40
700	54.78	29.26	1.077	38.91	18.80	2.09	14.09	1.69	23.81	9.02	60.60
800	57.61	29.94	1.181	43.51	18.75	2.38	13.65	1.85	25.25	8.36	56.58
900	59.29	30.15	0.645	43.53	18.64	2.72	13.23	2.14	28.31	8.34	55.83
1000	53.35	30.38	1.031	45.07	18.56	2.84	12.76	2.26	28.84	7.65	54.71